Science of the Total Environment 595 (2017) 2–12

Contents lists available at ScienceDirect

Science of the Total Environment

journal homepage: www.elsevier.com/locate/scitotenv

Estimation of CO_2 reduction by parallel hard-type power hybridization for gasoline and diesel vehicles

Yunjung Oh [a], Junhong Park [b], Jong Tae Lee [b], Jigu Seo [a], Sungwook Park [c,*]

[a] Graduated School of Hanyang University, Seoul 133-791, Republic of Korea
[b] National Institute of Environmental Research, Incheon 404-708, Republic of Korea
[c] School of Mechanical Engineering, Hanyang University, Seoul 133-791, Republic of Korea

HIGHLIGHTS

- ICEV and HEV models are developed based on vehicle and powertrain simulation tool.
- Fuzzy logic-based controller is implemented to generate HEV simulation models.4
- The prediction accuracy was validated by using a chassis dynamometer test data.
- Hybrid system can improve the fuel efficiency of ICEVs especially in city modes.

GRAPHICAL ABSTRACT

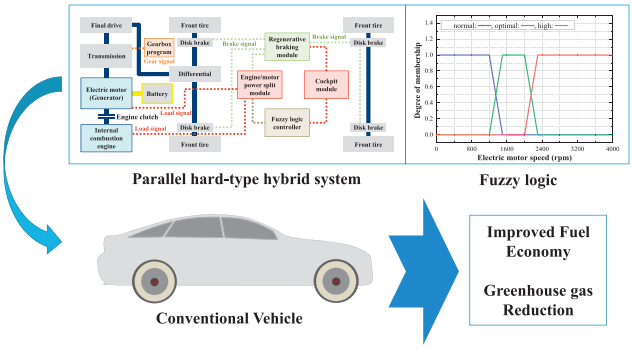

ARTICLE INFO

Article history:
Received 28 December 2016
Received in revised form 15 March 2017
Accepted 18 March 2017
Available online 31 March 2017

Editor: D. Barcelo

Keywords:
Vehicle dynamic based model
Fuzzy logic
Internal combustion engine vehicles (ICEVs)
Hybrid electric vehicles (HEVs)
Fuel efficiency
CO_2 emission rate

ABSTRACT

The purpose of this study is to investigate possible improvements in ICEVs by implementing fuzzy logic-based parallel hard-type power hybrid systems. Two types of conventional ICEVs (gasoline and diesel) and two types of HEVs (gasoline-electric, diesel electric) were generated using vehicle and powertrain simulation tools and a Matlab-Simulink application programming interface. For gasoline and gasoline-electric HEV vehicles, the prediction accuracy for four types of LDV models was validated by conducting comparative analysis with the chassis dynamometer and OBD test data. The predicted results show strong correlation with the test data. The operating points of internal combustion engines and electric motors are well controlled in the high efficiency region and battery SOC was well controlled within ±1.6%. However, for diesel vehicles, we generated virtual diesel-electric HEV vehicle because there is no available vehicles with similar engine and vehicle specifications with ICE vehicle. Using a fuzzy logic-based parallel hybrid system in conventional ICEVs demonstrated that HEVs showed superior performance in terms of fuel consumption and CO_2 emission in most driving modes.

1. Introduction

The dependency on fossil fuels as well as the related environmental problems induced by greenhouse gas (GHG) emissions has recently become an issue. Leading climate alarmists have been insisting that GHG

* Corresponding author at: School of Mechanical Engineering, 222 Wangsimni-ro, Seongdong-gu, Seoul 133-791, Republic of Korea.
E-mail address: parks@hanyang.ac.kr (S. Park).

http://dx.doi.org/10.1016/j.scitotenv.2017.03.171
0048-9697/

Nomenclature

API	Application programming interface
DF	Degree of fulfillment
EIA	Energy information administration
FLC	Fuzzy logic based controller
GHG	Greenhouse gas
GVW	Gross vehicle weight
HEVs	Hybrid electric vehicles
HIL	Hardware-in-the-Loop
HWFET	Highway fuel economy test cycle
ICCT	International Council on Clean Transportation
ICE	Internal combustion engine
IPCC	Intergovernmental Panel on Climate Change
LDVs	Light-duty vehicles
MBD	Millions of barrels per day
NIER	National institute of environmental research
NREL	National renewable energy laboratory
R^2	Determination coefficients

emissions need to be reduced by 50–80% compared to the present level in order to prevent serious catastrophic climate changes (Çağatay Bayindir et al., 2011; Leighty et al., 2012). However, it is hard to achieve drastic GHG emission reduction because fossil fuels are still the dominant energy resource worldwide (Yeatman, 2009). The US energy information administration (EIA) group estimates that global oil consumption in 2015 was 93 million barrels per day (MBD) and more than half of oil is consumed by the transportation sector (Energy Information Administration (EIA), 2014; Kodjak, 2011). The International Council on Clean Transportation (ICCT) and the Intergovernmental Panel on Climate Change (IPCC) research groups estimated that more than half of global oil products are consumed and 23% of global anthropogenic CO_2 emissions are generated by the transportation sector (Kodjak, 2011; Edenhofer et al., 2014). Considering that internal combustion engine-based light-duty vehicles (LDVs) will continue to be common, future cars will need low emissions and high fuel efficiency along with good performance, safety, and reliability (Navigant Research, 2015; Taylor, 2010).

Implementation of hybrid systems in internal combustion engine vehicles (ICEVs) is a promising solution to satisfy both environmental requirements (reducing GHG emissions in the transportation sector) and customer demand for fuel efficiency (Katrašnik, 2009). A hybrid system first proposed by Chen et al. increases the powertrain energy conversion efficiency and eliminates needless fuel consumption and emissions generation while idle (Chan, 2002). In addition, regenerative braking embedded in a hybrid system can convert kinetic energy into electrical energy during deceleration. Considering that one third to one half of energy in conventional ICEVs is wasted as friction losses under urban driving conditions, a hybrid system is useful for improving fuel efficiency by recapturing wasted kinetic energy in ICEVs (Lv et al., 2015; Metz, 2013).

HEVs can be largely classified into three parts based on powertrain composition: series-, parallel, and a combination of parallel and series HEVs (Çağatay Bayindir et al., 2011). All these systems were designed to improve fuel efficiency and the vehicle driving performance. HEVs need additional electrical components (electric motor, battery pack, generator, embedded powertrain controller) compared with conventional ICEVs. For this reason, vehicle performances can vary because it is hard to develop optimized control logic with numerous variables (Katrašnik, 2009). The main challenge of HEVs is to design a robust powertrain control system.

Power train control strategies can be classified into rule-based and optimized method (Salmasi, 2007). Rule-based control strategies are designed using a load-leveling method (Hochgraf et al., 1996). The main role of the load-leveling method is to improve vehicle performance by shifting the operating points of the internal combustion engine and electric machine into an optimal area. Fuzzy rule-based and deterministic rule-based methods are included in the rule-based control strategy (Schouten et al., 2002; Lee and Sul, 1998). These methods are advantageous when implementing a real time supervisory control system. An optimization-based control strategy is designed to derive the maximum efficiency of the powertrain line while minimizing power losses based on cost. The control strategy can be classified into two categories: global optimization method and real time optimization (Amiri et al., 2009). The global optimization method is useful for minimizing the cumulative energy loss during all driving conditions, and the real time optimization method is useful for implementing a real time energy management system (Salmasi, 2007).

If possible, it is desirable to develop and advance HEV performance based on quantitative test data. However, it is impossible to develop HEVs only based on the chassis dynamometer or real driving tests because control logics and system configurations are highly complex. There are many variables that exist in an HEV system. Experimental approaches require large amounts of research resources compared to conventional ICEVs. For this reason, many vehicle simulation programs have been developed to reduce testing and increase research efficiency. Each simulation program uses different details for map and curve fitting data (Liao et al., 2004; Oh, 2005; Markel et al., 2002; Wipke et al., 1999). Performance of the powertrain line and motor characteristics of a HEV can be studied using the concept of Hardware-in-the-Loop (HIL) (Oh, 2005). ADVISOR, which was developed by the National Renewable Energy Laboratory (NREL), is (Markel et al., 2002) used to predict fuel economy, vehicle performance, and emissions. This program implements a combination of forward and backward approaches to reduce errors between the driver command and the actual response of the system components (Wipke et al., 1999). Mierlo and Maggetto proposed a loop iteration algorithm that is based on one global feedback loop to supplement a wickless of wheel to engine and backward simulation programs (Van Mierlo and Maggetto, 2004). Katrašnik investigated the forward facing simulation models for parallel hybrid powertrains and a conventional internal combustion engine powertrain (Katrašnik, 2007). The CO_2 emissions of electric vehicles were investigated using an AVL CRUISE vehicle and powertrain level simulation tool as well as the average CO_2 emissions data for generating electrical energy (Wahono et al., 2015).

In the present work, two types of conventional ICEVs (gasoline, diesel) and two types of parallel hard-type power HEV models (gasoline- and diesel-electric vehicle) are developed based on vehicle and powertrain simulation tool, which are based on backward-forwards approaches (AVL, 2011; Varga, 2013; Srinivasan and Kothalikar, 2009). A fuzzy logic-based controller (FLC) is implemented to generate virtual HEV models. The validity of the simulation results was verified by using the test data, and an FLC-based hybrid system is applied to conventional ICEVs to analyze the effectiveness of the powertrain hybridization on reducing fuel consumption and CO_2 emissions. Despite previous studies on prediction vehicle performances based on vehicle dynamic-based modeling, this work has some advantages for verifying the prediction accuracy of vehicle models by using extensive test data and predicting possible improvements in fuel efficiency when an FLC-based hybrid system is implemented in conventional ICEVs.

2. Modeling methodology

In the AVL CRUISE program, the dynamic-based vehicle simulation model is composed of 10–20 component modules (engine, transmission, torque converter, gearbox program, brake, tire, etc.). Compared to HEV, composing a vehicle and powertrain level simulation model for ICEV is relatively simple, as shown in Fig. 1.

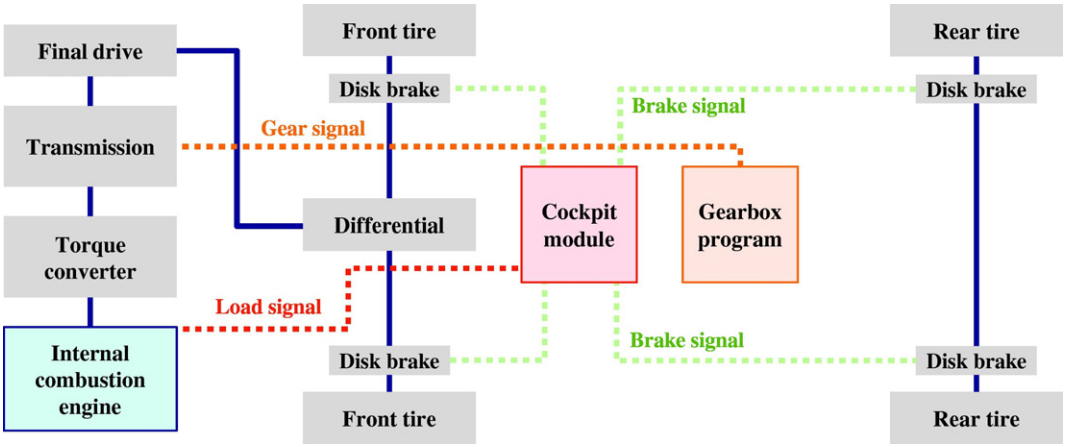

Fig. 1. Schematic diagram of a conventional ICEV (front-wheel drive).

Most vehicle components are linked as a mechanical connection. Cockpit and gearbox program modules are connected to the internal combustion engine (ICE). Gearbox and brake are linked as a data connection to control these modules at each time step. The operating condition of the vehicle is subject to driving resistance, which is determined as the sum of the tire rolling resistance, aerodynamic drag, and climbing resistance. To calculate a tire rolling resistance, vertical forces acting on the front and rear wheels should be calculated by using a momentum equilibrium equation. Basic vehicle dimension data used as an input for calculation and the resistance forces acting on the vehicle are illustrated in Fig. 2 (height of gravity center: $h_{V,DGC}$, distance between front and real axis: $l_{V,FR}$, horizontal distance between front axis and gravity center: $l_{V,DGC}$).

Based on Fig. 2, the governing equations of the vertical forces acting on wheels and total driving resistance force are defined as follows: (AVL, 2011; Srinivasan and Kothalikar, 2009)

$$F_{w,x,f,ax} = m_{V,act}\left[\left(1-\frac{l_{V,DGC,act}}{l_{V,FR}}\right)\cdot g\cdot \cos\alpha_U - \frac{h_{V,DGC,act}}{l_{V,FR}}\cdot(a_V + g\cdot \cos\alpha_U)\right] - F_{V,lift,f} \quad (1)$$

$$F_{w,x,r,ax} = m_{V,act}\left[\frac{l_{V,DGC,act}\cdot g\cdot \cos\alpha_U}{l_{V,FR}} + \frac{h_{V,DGC,act}}{l_{V,FR}}\cdot(a_V + g\cdot \sin\alpha_U)\right] - F_{V,lift,r} \quad (2)$$

$$F_{total,driving} = F_{accel} + F_{v,air} + F_{v,rr} + F_{incl} + F_{f,pt} \quad (3)$$

where $F_{w,x,f,ax}$ represents front axis load (N), $m_{V,act}$ represents instantaneous vehicle weight (kg), α_U represents inclination (rad), a_V represents vehicle acceleration (m/s^2), g represents gravitational acceleration (m/s^2), $F_{V,lift,f}$ represents a lift force of front tire (N), $F_{w,x,r,ax}$ represents rear axis load (N), and $F_{V,lift,r}$ represents lift force of rear tire (N). In addition, $F_{total,driving}$ represents the total driving force needed at each time step (N), F_{accel} is an acceleration force (N), $F_{v,air}$ is an air drag force (N), $F_{v,rr}$ is the tire rolling resistance force (N), F_{incl} is an inclination force (N), and $F_{f,pt}$ is the friction force generated in powertrain lines (N).

During the calculation process, the driving resistance is the main parameter to manipulate the operation conditions of power sources at each time step (engine or electric machine). To predict the performance and CO_2 emissions of parallel hybrid vehicles, fuzzy logic-based simulation models for HEVs were generated as shown in Fig. 3.

Compared to the structure of the ICEV model previously shown in Fig. 1, the parallel hard-type power hybrid vehicle model includes additional components such as electric motor, battery, regenerative braking module, engine clutch, and FLC module. The torque converter was eliminated to minimize power losses. The electric motor (generator) torque, power, and current are defined as a load signal and motor speed as follows:

$$T_{M,act} = T_{\max,curve}(n_{act}, V_{act})\cdot L_{signal,motor} \quad (4)$$

$$P_{M,act} = (T_{M,act}\cdot n_{act})\cdot \eta_M \cdot [2\pi/(60\cdot 9.80655)]\cdot(1/1000) \quad (5)$$

$$I_{M,act} = P_{M,act}/(V_{act}\cdot 1000) \quad (6)$$

where $T_{M,act}$ represents actual motor torque (Nm), $T_{\max,curve}$ represents maximum motor torque (Nm) defined as a function of motor speed (rpm, $n_{motor,act}$) and voltage (V, $V_{motor,act}$), and $L_{signal,motor}$ represents motor load signal (%), $P_{M,act}$ represents actual electric motor power (kW), η_M represents an energy efficiency of motor (%), and $I_{M,act}$ represents actual electric motor current (A).

The role of an electric motor in a parallel hard-type hybrid vehicle changes based on the vehicle operating state via either the controller, generator or the powertrain coupling. Considering that the thermal-

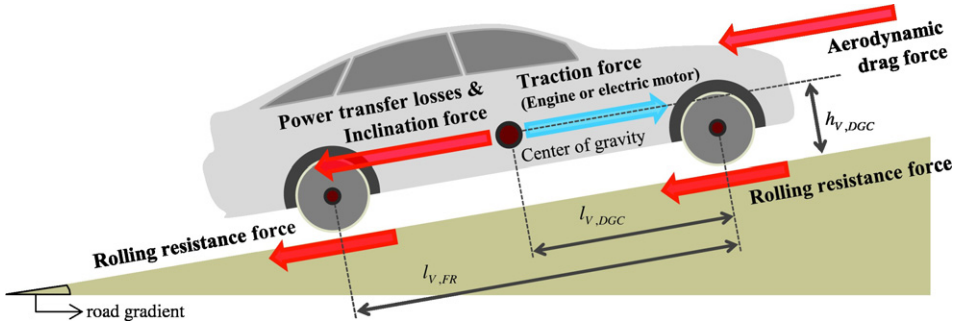

Fig. 2. Basic vehicle dimensions and forces acting on LDVs.

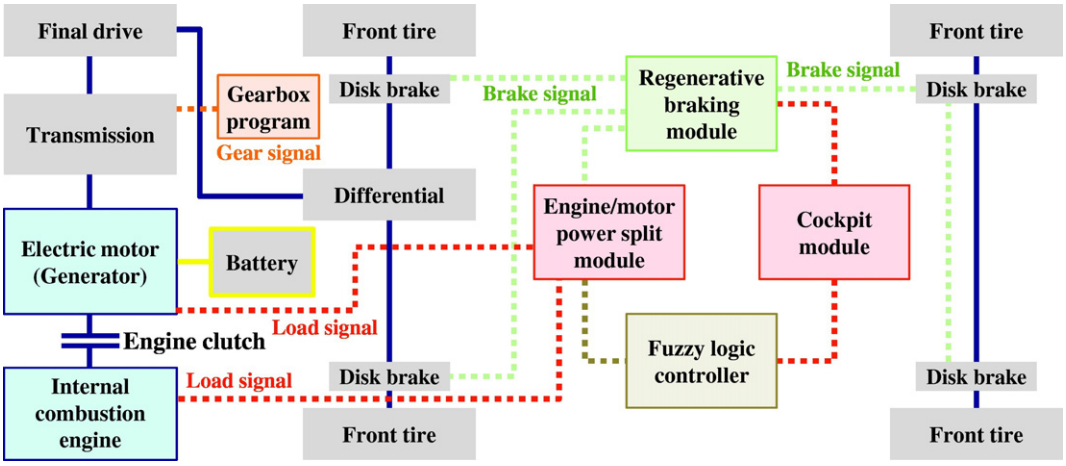

Fig. 3. Schematic diagram of a parallel type HEV (front-wheel drive).

temperature effect is not dominant in electric loss, the battery current is defined as a function of SOC as shown: (Nguyen et al., 2014)

$$I_{bat}(SOC_{bat}(t)) = \frac{V_{act}(SOC_{bat}(t)) - \sqrt{V_{act}^2(SOC_{bat}(t)) - 4 \cdot R_{bat} \cdot P_{bat}}}{2 \cdot R_{bat}} \quad (7)$$

where I_{bat} represents battery current (A), R_{bat} represents battery resistance (Ω), P_{bat} represents battery power (W), and $SOC_{bat}(t)$ represents battery SOC at specific time t (%).

The role of the FLC implemented in the HEV model is to derive a high-efficiency energy management strategy by considering operating conditions of vehicle components. In the FLC module, operating states of parallel hard-type hybrid vehicle are defined for the seven cases presented in Table 1.

where, $\mu_{toolow}(SOC)$, $\mu_{low}(SOC)$, $\mu_{normal}(SOC)$, and $\mu_{high}(SOC)$ represent when the degrees of membership of SOC in the fuzzy are set "too low", "low", "normal", and "high", respectively. $\mu_{normal}(T_{Desired})$ and $\mu_{high}(T_{Desired})$ represent the degrees of membership for the desired engine torque when the fuzzy are set "normal" and "high", respectively. $\mu_{low}(\omega_{EM})$, $\mu_{optimal}(\omega_{EM})$, and $\mu_{high}(\omega_{EM})$ represents the degrees of membership of the desired electric motor speed when the fuzzy logic is set to "low", "optimal" or "high".

Degree of fulfillment (DF) values which are proposed by Takagi and Sugeno are determined based on the membership functions as shown in Fig. 4. Based on membership functions, ICE and the electric motor operate over a high efficiency range while battery SOC is controlled in the range of 50 ± 3% (Takagi and Sugeno, 1985). Vehicle operating conditions for the total driving torque required for the vehicle, electric motor speed, and battery SOC condition data are transferred to the FLC module at each time step. The FLC module derives a consequence (generation torque) based on the average value of the degree of fulfillment of states 1 to 7, which is defined by the following equation:

$$N_c = \sum_{i=1}^{7} \left(DF_{state,i} \cdot c_{state,i}\right) / \sum_{i=1}^{7} DF_{state,i} \quad (8)$$

where, N_c represents the normalized controller output (Nm), $DF_{state,i}$ represents the DF value at state i, and $c_{state,i}$ represents the consequent value (Nm) at the state. Based on the degree of fulfillment values, operating conditions of ICE, electric motor, and battery are calculated at each time step.

When the battery SOC is too low, driving using the electric motor is avoided and the internal combustion engine generates the maximum torque to operate the vehicle and generates a maximum torque margin, which is transferred to the electric motor (generator) to charge up a low SOC battery quickly. The membership functions for the internal combustion engine were designed to operate an ICE in a low specific fuel consumption region.

From these processes, the FLC module calculates a desired instantaneous engine generation torque for each time step and transmits the operating signals to the final engine/motor power split module as a data connection. The engine/motor power split module generates a desired ICE and electric motor torque signal. In addition, this module determines a connection of the engine clutch condition. At each time step, the desired ICE and electric motor torque for parallel hard-type power hybrid vehicles are determined as follows: (Schouten et al., 2002)

(1). Low load condition (required total driving power < 10 kW & battery SOC is not too low)

$$T_{ICE} = 0, T_{EM} = T_{driving}$$

(2). Middle, high load condition (required power higher than 10 kW)

Table 1
Definition of FLC operating states for parallel hard-type hybrid vehicle (Schouten et al., 2002).

State	Operating condition			Generation torque (consequent)	Degree of fulfillment
	Battery SOC	Required total driving torque	Electric motor speed		
1	Too high	–	–	None	$\min(\mu_{high}(SOC)) = \mu_{high}(SOC)$
2	Normal	Normal	Optimal	20–30 Nm	$\min(\mu_{normal}(SOC), \mu_{normal}(T_{desired}), \mu_{optimal}(\omega_{EM}))$
3	Normal	–	Not optimal	None	$\min(\mu_{normal}(SOC), 1 - \mu_{optimal}(\omega_{EM}))$
4	Low	Normal	Low	10–15 Nm	$\min(\mu_{low}(SOC), \mu_{normal}(T_{desired}), \mu_{low}(\omega_{EM}))$
5	Low	Normal	Not low	30–45 Nm	$\min(\mu_{low}(SOC), \mu_{normal}(T_{desired}), 1 - \mu_{low}(\omega_{EM}))$
6	Too low	–	–	Max. generation	$\min(\mu_{too\ low}(SOC)) = \mu_{too\ low}(SOC)$
7	Not too low	High	–	None	$\min(1 - \mu_{too\ low}(SOC), \mu_{high}(T_{desired}))$

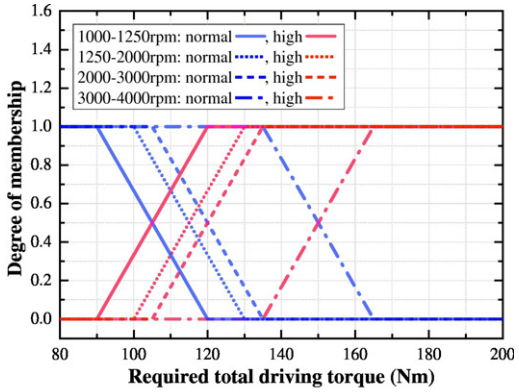

(a). Total traction force: gasoline-electric HEV

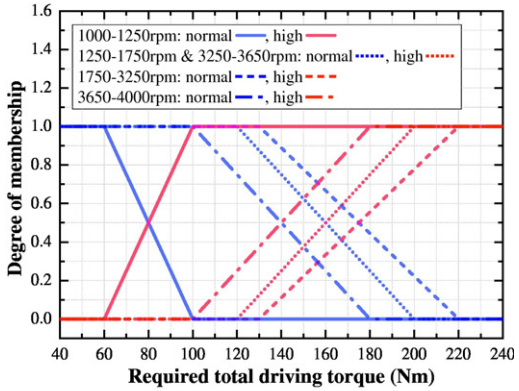

(b). Total traction force: diesel-electric HEV

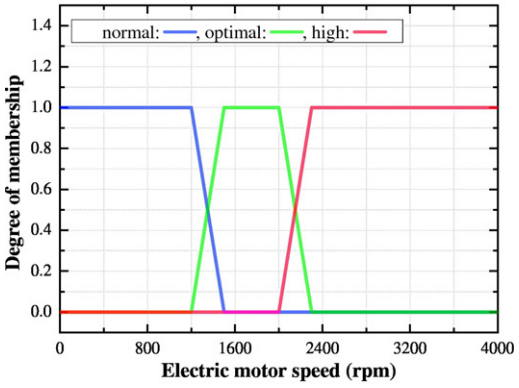

(c). Electric motor speed

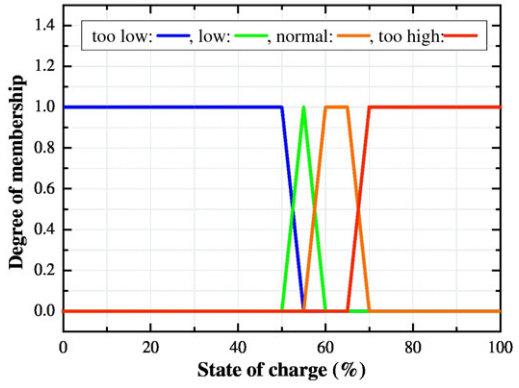

(d). Battery SOC

Fig. 4. Membership functions for total traction force, electric motor speed, and battery SOC (Schouten et al., 2002).

$$T_{ICE} = T_{driving} + T_{engine,gen}, T_{EM} = -T_{engine,gen}$$

(3). Regenerative braking condition

$$T_{ICE} = 0, T_{EM} = -T_{regen}$$

(4). SOC is too low (battery SOC is too low)

$$T_{ICE} = T_{driving} + T_{\max,gen}, T_{EM} = -T_{\max,gen}$$

Here, T_{ICE} represents the required engine torque (Nm), T_{EM} represents the required electric motor torque (Nm), $T_{driving}$ represents the required driving torque (Nm), $T_{engine,gen}$ represents the desired engine generation torque (Nm), T_{regen} represents the regenerative torque (Nm), and $T_{\max,gen}$ represents the maximum engine generation torque (Nm). The required driving power is calculated based on the required driving torque and rotational speed of the power source (ICE or electric motor) as:

$$P_{V,req} = 2\pi \cdot T_{driving} \cdot \omega_{E/M} \cdot (60/1000) \quad (9)$$

where $P_{V,req}$ represents the required driving power (kW) and $\omega_{E/M}$ represents the rotational speed (rad/s) of the power source.

3. Computational test conditions

In this study, four types of LDV simulation models (gasoline, diesel, gasoline-electric, and diesel-electric) are developed based on vehicle and powertrain simulation tools. Some experimental data such as fuel efficiency, CO_2 emission rate, and engine speed are implemented to validate the prediction accuracy of the simulation models. Detailed specifications of LDVs are described in Table 2.

The Diesel HEV model was an artificially generated model based on the Diesel ICE model using hybrid systems presented in this paper (electric motor, battery, engine clutch and FLC module). The gross vehicle weight of the HEV B model is determined to be 1995 kg assuming that the weight of the hybrid systems is 200 kg (weight of the Diesel ICE model: 1775 kg). The initial battery SOC condition of Gasoline HEV and Diesel HEV model is defined as 51%.

Meanwhile, the FTP-75 mode, highway fuel economy test cycle (HWFET) and six types of the national institute of environmental research (NIER, Korea) driving modes (NIER03, NIER05, NIER07, NIER09, NIER12 and NIER14) are implemented to analyze fuel efficiency and CO_2 emission rates of LDVs under various driving conditions. From previous research, it is known that velocity and acceleration distribution of

Table 2
Specifications of four types of LDVs.

Specifications	Gasoline ICE	Diesel ICE	Gasoline HEV	Diesel HEV (virtual model)
Empty vehicle weight (kg)	1415	1775	1595	1995
Engine displacement (cc)	1999	2199	1999	2199
Max. power (PS)	172	202	156	202
Max. torque (kg·m)	20.5	45	19.3	45
Number of cylinder (−)	4	4	4	4
Number of gear (−)	6	6	6	6
Energy source	Gasoline	Diesel	Gasoline-electric	Diesel-electric
Dimensions				
Height (m)	1.470	1.470	1.475	1.470
Width (m)	1.825	1.860	1.865	1.860

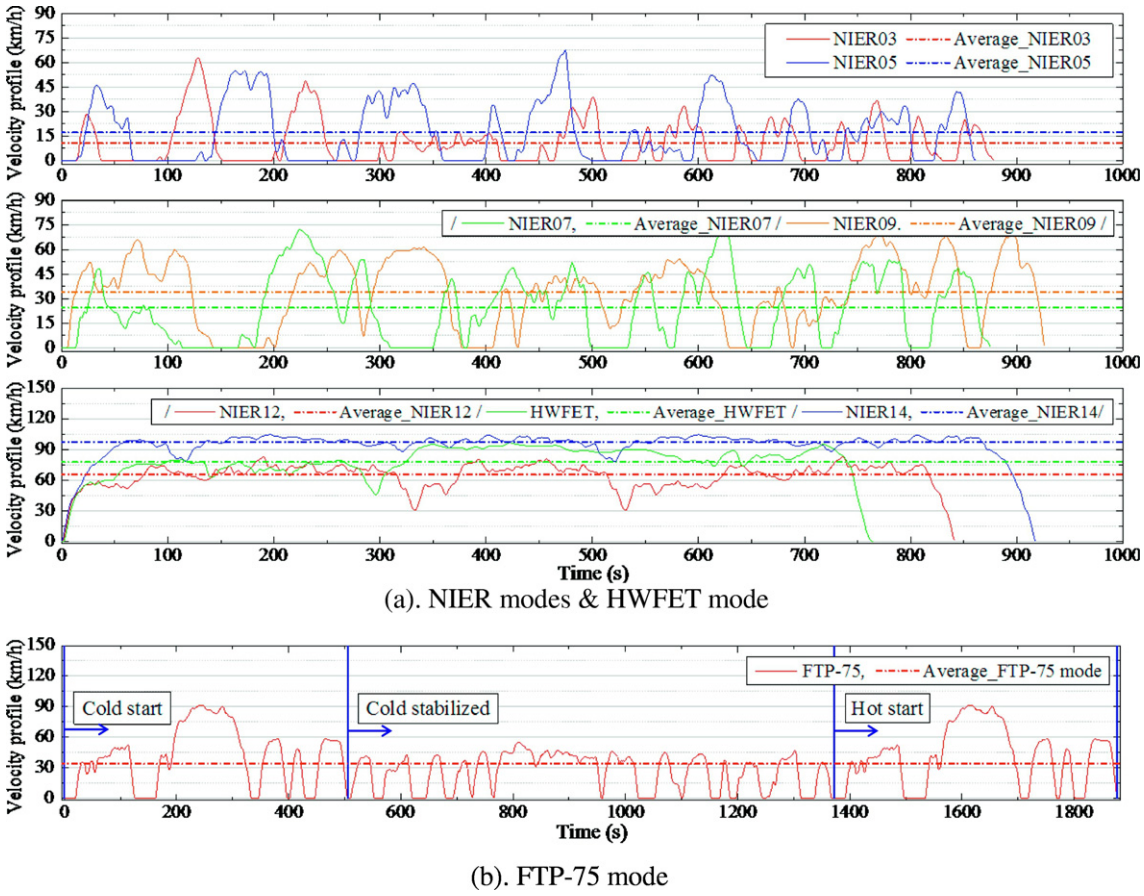

Fig. 5. Eight types of velocity profiles.

the NIER modes reflect the domestic real driving patterns in Korea (Park et al., 2011). The FTP-75 mode contains a cold start condition. However, the cold start regime is not considered and all test modes selected in this study assumed that the vehicle started in a hot start condition. Detailed velocity profiles of the FTP-75, HWFET, and NIER modes are shown in Fig. 5 and simulation cases are summarized in Table 3.

4. Results and discussion

4.1. Verifying the prediction accuracy of LDV models with compared to chassis dynamometer test data

In previous research, the relationship between the pedal sensor position and engine torque was investigated and implemented in the gear shifting logic (Oh et al., 2014). The present study also considers this relationship for the vehicle dynamic models to improve the prediction accuracy of the engine operating condition.

To validate the prediction accuracy of the instantaneous engine speed, comparative analysis between measured data that is acquired using on-board diagnostics (OBD) signals and simulation data was conducted as shown in Fig. 6. If the predicted engine speed shows a distinct deviation compared to the test data, the gear shifting model or road load setting should be modified to predict an accurate gear position in the same time window.

Table 3
Simulation cases for predicting fuel efficiency and CO_2 emission rate of ICEVs and HEVs.

Vehicle types	Driving modes
Gasoline ICE	FTP-75 mode: 3-phase
Diesel ICE	HWFET mode
Gasoline HEV (virtual model)	Six type of NIER modes (NIER 03, 05, 07, 09, 12, and 14)
Diesel HEV (virtual model)	
4 cases	8 cases
Total 32 cases	

In case of conventional ICEVs (Gasoline ICE and Diesel ICE models), it is revealed that predicted engine speed data has strong correlation with experimental results regardless of driving mode. The trend line almost overlaps with the ideal line, and determination coefficients (R^2) converged in the range 0.8–0.9. In the case of the Gasoline HEV model, the overall engine speed prediction results are similar to the test data. It is hard to directly compare predicted results of the Gasoline HEV model with test results because the power control logic is not the same as that of the actual vehicle, even if the major specification is entered identically in the simulation. However, it is meaningful to validate whether the vehicle dynamic model for Gasoline HEV can predict reasonable calculation results. Considering that the maximum charging/discharging efficiency of a battery implemented in the Gasoline HEV model is when SOC control is 50%, it is essential to control a SOC in a specific range to minimize battery charging/discharging losses. From this point of view, the membership function for the battery is well designed because the SOC is in the 50 ± 3% range during all driving. From this procedure, prediction accuracy of the engine speed of three types of LDVs (Gasoline ICE, Diesel ICE and Gasoline HEV) is validated and adaptation of the FLC module is adequate to describe actual HEV performance.

To evaluate the stability of the fuzzy logic-based battery management strategy in HEVs, the battery SOC change rate between when the vehicle starts and finishes the driving course is predicted as shown in Fig. 7. The results show that SOC deviation does not exceed 1.6% regardless of vehicle type and driving mode (maximum battery SOC change rate – Gasoline HEV: 1.41% Diesel HEV: 1.59%). From

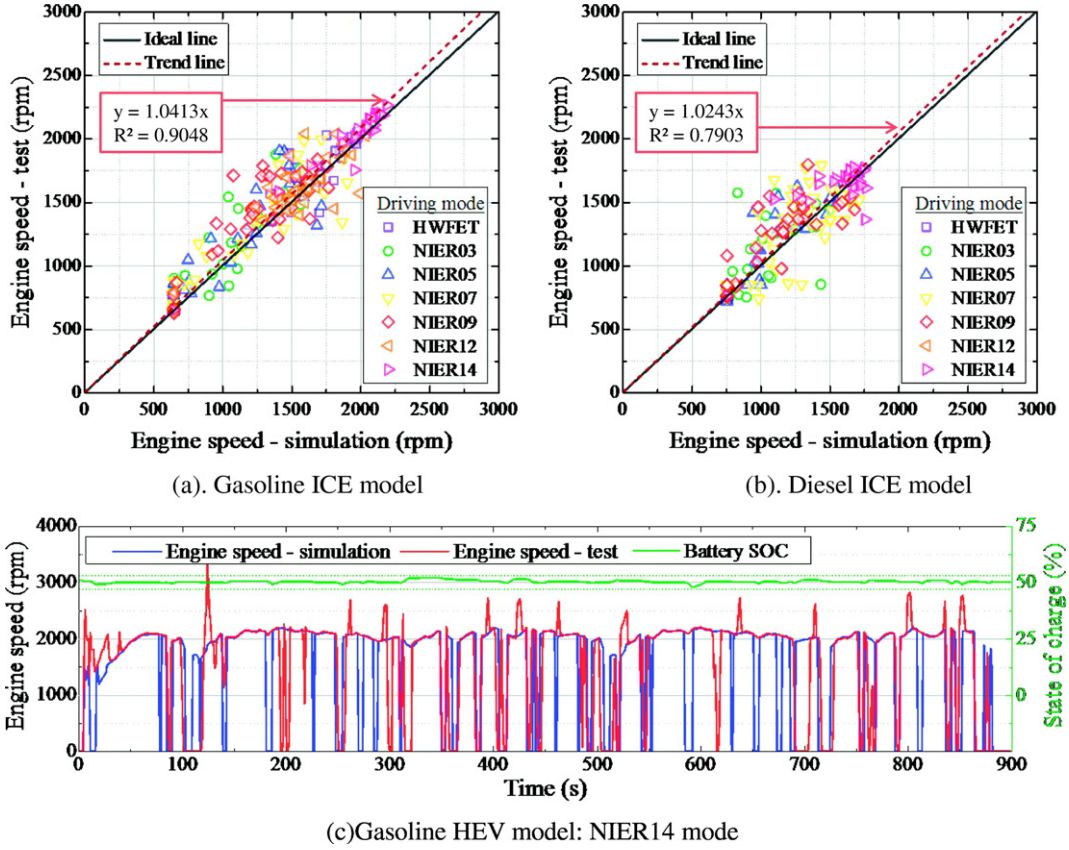

Fig. 6. Analyzing an engine speed correlations between test and simulation data.

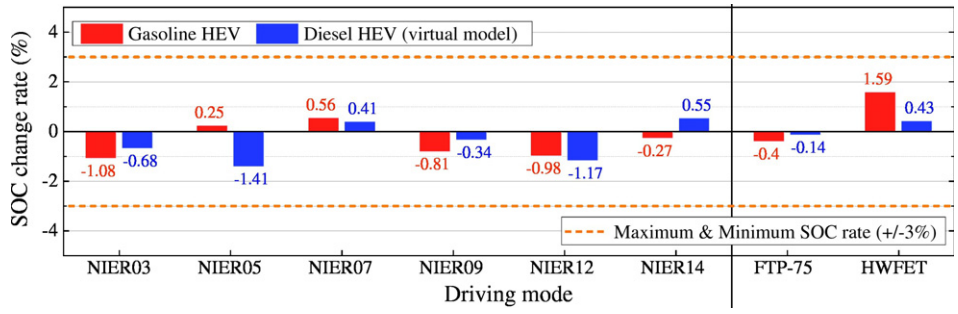

Fig. 7. Predicted SOC change rate between when the vehicle starts and finishes the driving course.

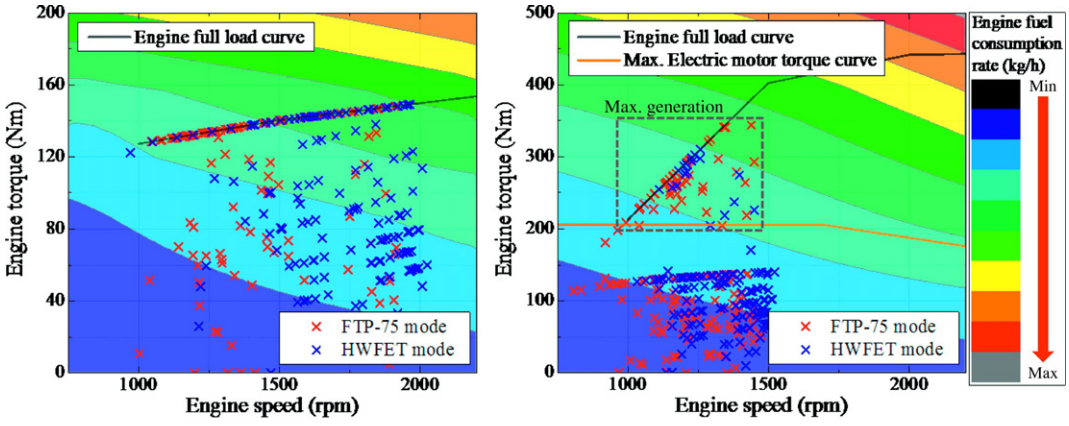

Fig. 8. Operating points of the internal combustion engine in FTP-75 and HWFET mode.

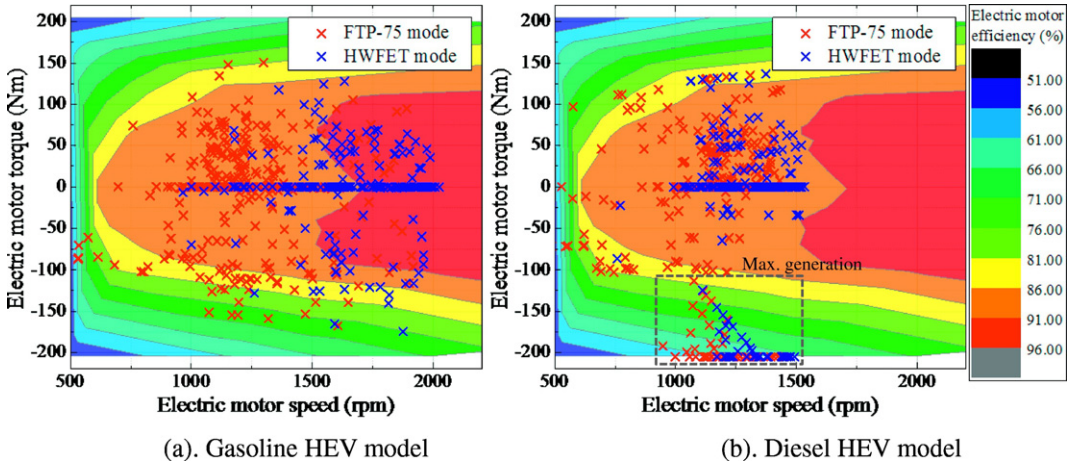

Fig. 9. Operating points of the electric motor in FTP-75 and HWFET mode.

these results, it is apparent that Gasoline HEV and Diesel HEV models can satisfy the requirement that battery SOC deviation between vehicle start and end status should not exceed 3% in the chassis dynamo test. This procedure is important to understand the accumulated results such as fuel efficiency and CO_2 emission because a battery SOC condition can influence the fuel efficiency of HEVs.

4.2. Investigation of the engine and electric motor operating conditions: HEVs

To confirm that the FLC module is adequately operating in HEV models (Gasoline HEV, Diesel HEV), the operating points of the engine and electric motor in FTP-75 and HWFET modes are predicted and presented as shown in Figs. 8 and 9.

In the Gasoline HEV model (energy source: gasoline-electric), the operating points of the gasoline engine are included on the engine full load curve because the membership function for the gasoline engine is designed to utilize high load conditions to reduce specific fuel consumption (g/kWh) as previously shown in Fig. 4(a). The remaining engine torque (defined as the gap between the maximum engine torque and required torque to operate a vehicle) is transferred to the electric motor to generate electric energy. Most operating points of the electric motor are concentrated in the high efficiency region. The overall energy conversion efficiency (kinetic to electric energy) of the Gasoline HEV model is expected to be high.

In the Diesel HEV model (energy source: diesel-electric), on the other hand, engine operating points are concentrated at the low load condition because the engine full load curve is formed in the 200–450 Nm range, which is much higher than the general traction torque range needed to operate the vehicle. For this reason, a large portion of the engine's torque can be transferred to an electric motor if the diesel engine generates maximum torque to convert needless kinetic energy into electric energy. However, the energy conversion efficiency of the electric motor sharply decreases when the motor generation torque is higher than 100 Nm. For this reason, it is desirable to generate adequate torque in the diesel engine to reduce heat loss in the energy conversion process.

On the whole, the FLC module implemented in this study shows good performance at concentrating the operating points of the internal combustion engine and electric motor in the high efficiency range. In the HEV B model, it is predicted that a small portion of engine operating points are concentrated on the full load curve even if the energy conversion efficiency is too low to recover a battery SOC in a short time.

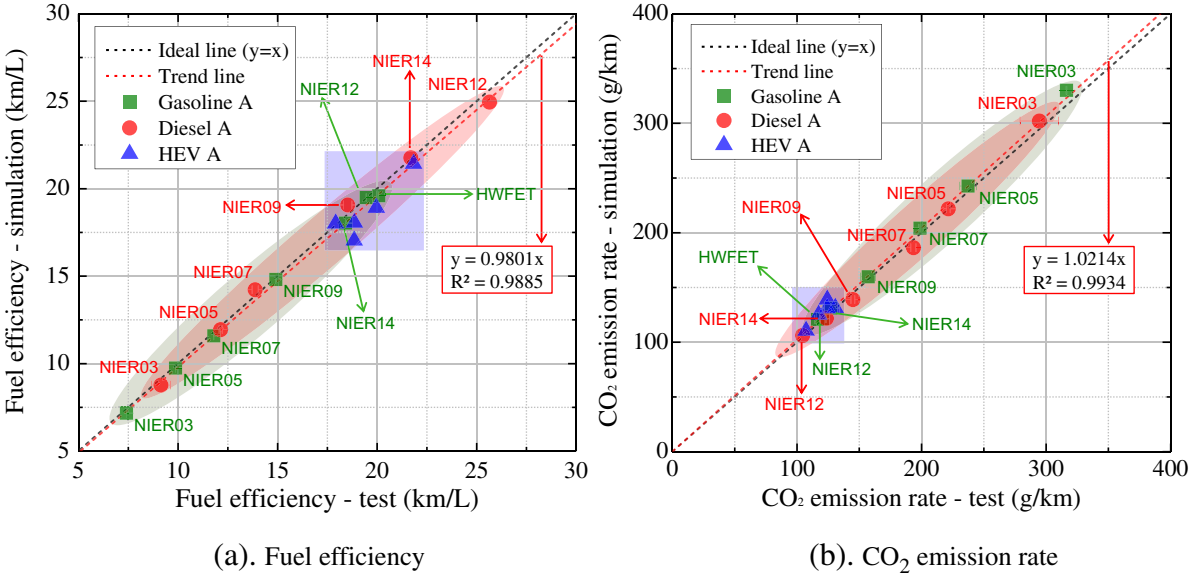

Fig. 10. Verification of the prediction accuracy of fuel efficiency and CO_2 emission.

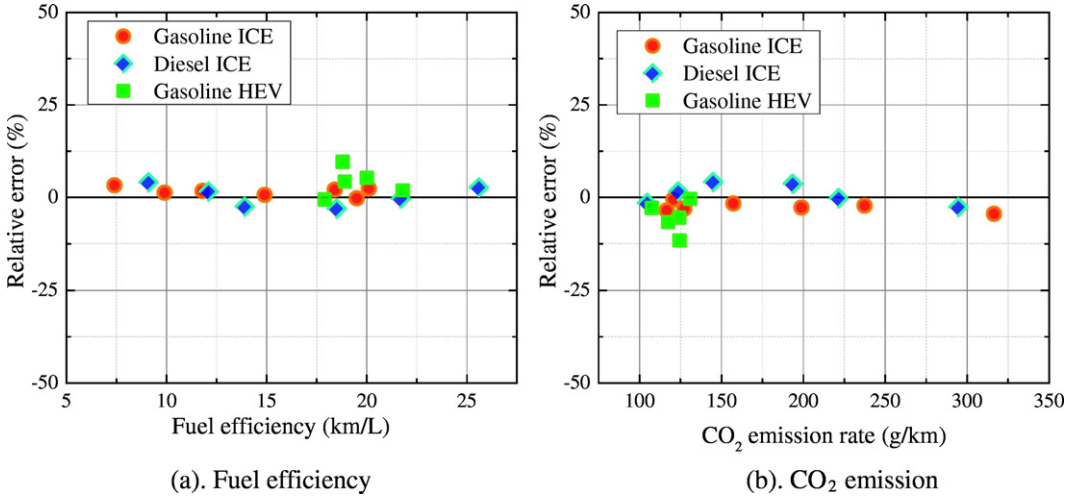

Fig. 11. Relative error of the tested and predicted result.

4.3. Prediction of fuel efficiency and CO_2 emission rate of ICEVs and HEVs

Fig. 10 shows the predicted fuel efficiency and CO_2 emission rate of three types of LDVs. Except for virtual model (Diesel HEV), comparative analysis is conducted by using the chassis dynamometer test data to validate the prediction accuracy. It is hard to directly compare the tests and predicted results of the Gasoline HEV model because the power control logic is not the same as that of the vehicle even if the major specification is set to be the same.

The predicted results show a strong correlation with the test data. The gradient of the trend lines is almost the same as the gradient of the ideal lines. The determination coefficients (R2) are also converged at 0.99. All prediction results and relative errors of the four types of LDVs are presented in Fig. 11.

As shown in the results, fuel efficiency and CO_2 emission rate of the conventional ICEV models are highly dependent on the driving mode. Gasoline ICE and Diesel ICE models consume almost three times as much fuel when driving in NIER03 mode compared to HWFET. On the other hand, the fuel efficiency and CO_2 emission rates of the HEV models do not exhibit a distinct deviation regardless of the driving mode because the regenerative braking system, idling stop system and high efficiency of the electric motor at low speed mode compensate for losses in city mode.

Figs. 12 and 13 show fuel efficiency and CO_2 emission rates of the ICEVs and HEVs to analyze vehicle performance improvement when applying the FLC-based hybrid system. Four LDVs were classified into two categories based on the fuel type of the ICE as Gasoline ICE–Gasoline HEV and Diesel ICE–Diesel HEV.

As expected, HEVs show superior performance. The improvement in the fuel efficiency is 4.8–152.1% and the reduction in the CO_2 emission rate is 4.6–60.3% when applying a hybrid system in the Gasoline ICE model. This trend is also shown in the Diesel ICE – Diesel HEV group. After implementing the FLC-based hybrid system in the Diesel ICE model, fuel efficiency is improved by 27.2–72.7% and the CO_2 emission rate is reduced by 21.4–42.1% at low driving speeds. However, these advantages of fuel efficiency and CO_2 emission are

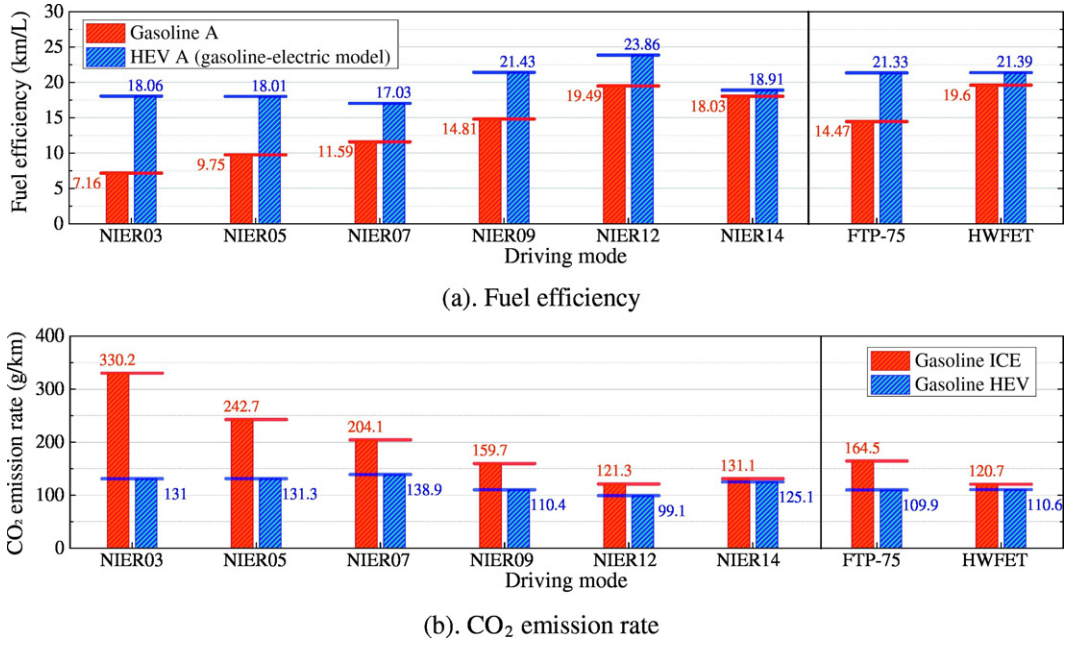

Fig. 12. Comparative analysis of the fuel efficiency and CO_2 emission: Gasoline ICE and Gasoline HEV.

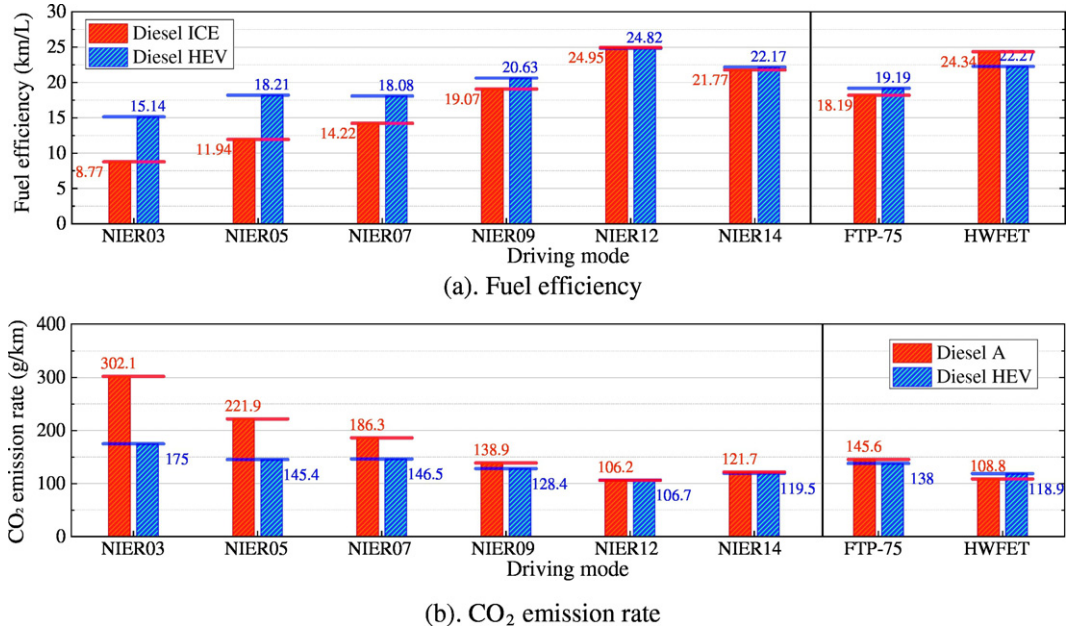

Fig. 13. Comparative analysis of the fuel efficiency and CO_2 emission: Diesel ICE and Diesel HEV.

gradually decreased as the average speed of driving mode is increased. At high speeds, the effects of regenerative braking and the engine stop at idle condition is reduced because the stop and acceleration conditions for high speed modes (NIER09, NIER12, NIER14 and HWFET) differ from those of low speed modes (NIER03, NIER 05, NIER07 and NIER09). Moreover, the fuel efficiency of a diesel car is relatively higher than that of a gasoline car due to a high engine compression ratio. For this reason, it is predicted that the fuel efficiency of the Diesel ICE model is superior to that of the HEV B model in HWFET mode (average speed: 77.6 km/h).

The overall simulation results show a potential improvement in the fuel efficiency by implementing an FLC-based hybrid system in conventional ICEVs. However, some advanced technologies such as engine downsizing, reduction in gross vehicle weight (GVW), adaptation of planetary gear or optimization of the membership function of the FLC module are required to advance the fuel efficiency of the HEV B model in high speed modes.

5. Conclusion

In this study, the CO2 reduction is estimated when the FLC-based hybrid system is implemented on conventional ICEVs. Powertrain level simulation tools (AVL CRUISE) was used to calculate CO2 emission factors of vehicle and four types of vehicle simulation models were developed. (Gasoline ICE, Diesel ICE, Gasoline HEV, Diesel HEV).

The accuracy of the simulation model was validated by comparing the simulation result with the chassis dynamometer test result. The trend lines are similar to the ideal line, and determination coefficients (R^2) are higher than 0.8. It was also revealed that the battery SOC is well managed in the range of target value ($50 \pm 1.6\%$) for both Gasoline HEV and Diesel HEV models regardless of driving mode.

In comparative analysis between ICEVs and HEVs, the operating points of the ICEVs are scattered without specific trends, but, those of HEVs are concentrated in high fuel economy region. The results showed that Gasoline HEV improved fuel efficiency by 4.8–152.1% compared to conventional gasoline ICEV and Diesel HEV improved 27.2–72.7% than conventional Diesel ICEV. The CO_2 emissions of Gasoline HEV and Diesel HEV were reduced by up to 60.3% and 42.1% respectively, compared to the conventional ICEV.

Acknowledgments

The support of the research work presented in this paper by AVL List GmbH in providing licenses of AVL CRUISE within the frame of its University Partnership Program and the Korea Institute of Energy Technology Evaluation and Planning (KETEP) and the Ministry of Trade, Industry & Energy (MOTIE) of the Republic of Korea (No. 20164010200860).

Reference

Amiri, M., Esfahanian, M., Hairi-Yazdi, M.R., Esfahanian, V., 2009. Minimization of power losses in hybrid electric vehicles in view of the prolonging of battery life. J. Power Sources 190, 372–379.
AVL, 2011. Users Guide Book. AVL CRUISE Version 2011.2.05.
Çağatay Bayindir, K., Gözüküçük, M.A., Teke, A., 2011. A comprehensive overview of hybrid electric vehicle: powertrain configurations, powertrain control techniques and electronic control units. Energy Convers. Manag. 52, 1305–1313.
Chan, C., 2002. The state of the art of electric and hybrid vehicles. Proc. IEEE 90, 247–275.
Edenhofer, O., Pichs-Madruga, R., Sokona, Y., Farahani, E., Kadner, S., Seyboth, K., Adler, A., Baum, I., Brunner, S., Eickemeier, P., 2014. Climate Change 2014: Mitigation of Climate Change. Working Group III Contribution to the Fifth Assessment Report of the Intergovernmental Panel on Climate Change.
Energy Information Administration (EIA), 2014. Short-Term Energy Outlook (STEO): Independent Statistics & analysis report for the US.
Hochgraf, C.G., Ryan, M.J., Wiegman, H.L., 1996. Engine Control Strategy for a Series Hybrid Electric Vehicle Incorporating Load-Leveling and Computer Controlled Energy Management. SAE International.
Katrašnik, T., 2007. Hybridization of powertrain and downsizing of IC engine – a way to reduce fuel consumption and pollutant emissions – part 1. Energy Convers. Manag. 48, 1411–1423.
Katrašnik, T., 2009. Analytical framework for analyzing the energy conversion efficiency of different hybrid electric vehicle topologies. Energy Convers. Manag. 50, 1924–1938.
Kodjak, D., 2011. Policies to Reduce Fuel Consumption, Air Pollution, and Carbon Emissions From Vehicles in G20 Nations. International Council on Clean Transportation (ICCT).
Lee, H.D., Sul, S.K., 1998. Fuzzy-logic-based torque control strategy for parallel-type hybrid electric vehicle. IEEE Trans. Ind. Electron. 45, 625–632.
Leighty, W., Ogden, J.M., Yang, C., 2012. Modeling transitions in the California light-duty vehicles sector to achieve deep reductions in transportation greenhouse gas emissions. Energ. Policy 44, 52–67.
Liao, G., Weber, T., Pfaff, D., 2004. Modelling and analysis of powertrain hybridization on all-wheel-drive sport utility vehicles. Proc. Inst. Mech. Eng. D J. Automobile Eng. 218, 1125–1134.
Lv, C., Zhang, J., Li, Y., Yuan, Y., 2015. Mechanism analysis and evaluation methodology of regenerative braking contribution to energy efficiency improvement of electrified vehicles. Energy Convers. Manag. 92, 469–482.
Markel, T., Brooker, A., Hendricks, T., Johnson, V., Kelly, K., Kramer, B., et al., 2002. ADVISOR: a systems analysis tool for advanced vehicle modeling. J. Power Sources 110, 255–266.

Metz, L.D., 2013. Potential for Passenger Car Energy Recovery Through the Use of Kinetic Energy Recovery Systems (KERS). SAE International.
Navigant Research, 2015. Transportation Forecast Light Duty Vehicles: Light Duty Stop-start, Hybrid Electric, Plug-in Hybrid Electric, Battery Electric, Natural Gas, Fuel Cell, Propane Autogas, and Conventional Vehicles: Global Market Forecasts.
Nguyen, A., Lauber, J., Dambrine, M., 2014. Optimal control based algorithms for energy management of automotive power systems with battery/supercapacitor storage devices. Energy Convers. Manag. 87, 410–420.
Oh, S.C., 2005. Evaluation of motor characteristics for hybrid electric vehicles using the hardware-in-the-loop concept. IEEE Trans. Veh. Technol. 54, 817–824.
Oh, Y., Park, J., Lee, J., Eom, M.D., Park, S., 2014. Modeling effects of vehicle specifications on fuel economy based on engine fuel consumption map and vehicle dynamics. Transp. Res. Part D: Transp. Environ. 32, 287–302.
Park, J., Lee, J., Lee, T., Lee, T., Choi, K., Lee, Y., 2011. Reflecting real world driving condition for vehicle emission test modes. Kor. Soc. Atmos. Environ. 66.
Salmasi, F.R., 2007. Control strategies for hybrid electric vehicles: evolution, classification, comparison, and future trends. IEEE Trans. Veh. Technol. 56, 2393–2404.
Schouten, N.J., Salman, M.A., Kheir, N.A., 2002. Fuzzy logic control for parallel hybrid vehicles. IEEE Trans. Control Syst. Technol. 10, 460–468.
Srinivasan, P., Kothalikar, U.M., 2009. Performance Fuel Economy and CO_2 Prediction of a Vehicle using AVL Cruise Simulation Techniques. SAE International.
Takagi, T., Sugeno, M., 1985. Fuzzy identification of systems and its applications to modeling and control. IEEE Trans. Syst. Man Cybern. 116–132.
Taylor, P., 2010. Energy Technology Perspectives 2010: Scenarios & Strategies to 2050. 7. International Energy Agency (IEA), pp. 255–276.
Van Mierlo, J., Maggetto, G., 2004. Innovative iteration algorithm for a vehicle simulation program. IEEE Trans. Veh. Technol. 53, 401–412.
Varga, B.O., 2013. Electric vehicles, primary energy sources and CO_2 emissions: Romanian case study. Energy 49, 61–70.
Wahono, B., Santoso, W.B., Nur, A., 2015. Analysis of range extender electric vehicle performance using vehicle simulator. Energy Procedia 68, 409–418.
Wipke, K.B., Cuddy, M.R., Burch, S.D., 1999. ADVISOR 2.1: A user-friendly advanced powertrain simulation using a combined backward/forward approach. IEEE Trans. Veh. Technol. 48, 1751–1761.
Yeatman, W., 2009. Global Warming 101: Costs.